Sorting lithium-ion battery electrode materials using dielectrophoresis at frequencies of up to 500 kHz

Jasper Giesler,[†] Laura Weirauch,[†] Alica Rother,[‡] Jorg Thöming,[†,‡] Georg R. Pesch,[*,¶,§] and Michael Baune[†,‡,§]

[†]*Chemical Process Engineering, Faculty of Production Engineering, University of Bremen, Bremen, Germany*

[‡]*Center for Environmental Research and Sustainable Technology (UFT), University of Bremen, Bremen, Germany*

[¶]*University College Dublin, School of Chemical and Bioprocess Engineering, Dublin, Ireland*

[§]*Both authors contributed equally to this work.*

E-mail: georg.pesch@ucd.ie

Abstract

Lithium-ion batteries (LIBs) are common in everyday life and the demand for their raw materials is increasing. Additionally, spent LIBs should be recycled for achieving a circular economy and supply resources for new LIBs or other products. Especially the recycling of the active material of the electrodes is in the focus of current research. Existing approaches for the recycling (e.g., pyro-, hydrometallurgy or flotation) still have their drawbacks, such as the loss of material, generation of waste, or lack of selectivity. In this study, we test the behavior of commercially available $LiFePO_4$

and two types of graphite microparticles in a dielectrophoretic high-throughput filter. Dielectrophoresis is a volume dependent electrokinetic force that is commonly used in microfluidics but recently also for applications that focus on enhanced throughput. In our study, graphite particles show significantly higher trapping than $LiFePO_4$ particles. The results indicate that nearly pure fractions of $LiFePO_4$ can be obtained with this technique from a mixture with graphite.

Introduction

Lithium-ion batteries (LIBs) power electrical devices in nearly all parts of modern society. For example, LIBs are used in portable electronics and electric vehicles. Consequently, the demand for LIB resources grows.[1] To recover materials of spent LIBs, the recycling of electrodes is a focus of current research. As about one half of the weight of LIBs consists of the active material of anode and cathode, their recycling is desirable.[2] Cathode active materials typically are lithium metal oxides (e.g., $LiCoO_2$, $LiFePO_4$ or $LiNi_{1/3}Mn_{1/3}Co_{1/3}O_2$), whereas graphite is common for anodes.[1,2] Anode and cathode consist, among carbon black as conductive additive and a polymer binder, of a current collector (Cu or Al foil) to which the active material adheres.[2–4] Current collector and active material can be separated by both, chemical and mechanical approaches, such as crushing and sieving.[1,3–5] Typically, one product of these processes is the so-called black mass, a mixture from anode and cathode active material.[4] Current recycling techniques for black mass are, for example, pyro- or hydrometallurgical and focus on the recovery of cathode active material because of its higher value compared to graphite. Graphite might be lost or burned as energy source within the recycling process.[1,2,5–7] Yet processes exist where graphite can be recovered. In hydrometallurgical approaches, the lithium metal oxides are dissolved in acid during a leaching step and recovered in subsequent unit operations. Graphite can simply be recovered by filtration after the leaching step.[4] But as significant amounts of liquid wastes are produced in this recycling pathway[8] it would benefit from an efficient sorting step before the leaching to reduce the

amount of chemicals needed. As the active materials are essentially microparticles,[9–11] direct recycling using particle separation techniques could play a vital role within the recycling process to enhance or replace existing recycling approaches of LIBs. One approach which is well established for particulate systems and capable of handling large amounts of product is flotation, which was also applied to separate black mass. This works because anode and cathode material show different wettability.[5,7,12–14] However, according to Neumann et al.,[4] the process needs to be optimized further as the achievable recovery rates are currently too low.

This paper focuses on developing a novel mechanical approach for separating black mass using dielectrophoresis (DEP). DEP is the movement of a polarizable particle in an inhomogeneous electric field. Usually, it is used in the biomedical field and primarily in microfluidic devices.[15,16] Although DEP is label-free, has high selectivity, and the capability of addressing nano- to micrometer-scaled particles,[17–19] few studies addressed recycling or the throughput that would be required for this.[20–25] By using a setup based on printed circuit boards (PCBs), we assess the behavior of $LiFePO_4$ and graphite microparticles and their mixture under the influence of DEP. To the best of the authors' knowledge the separation of LIB electrode material using dielectrophoresis has not yet been addressed. This study aims to serve as a starting point for future research in this field by describing the possibilities and limitations of DEP as a separation technique for these materials.

Materials and Methods

Dielectrophoretic separator

The separator used in this study is an updated version of the one which was evaluated and published in Ref. 23 and is designed to selectively trap particles when an electric field is applied. An overview of the device can be seen in Figure 1. The key feature of this device are two inexpensive (< 1€/pc.) custom designed PCBs (manufactured by JiaLiChuang

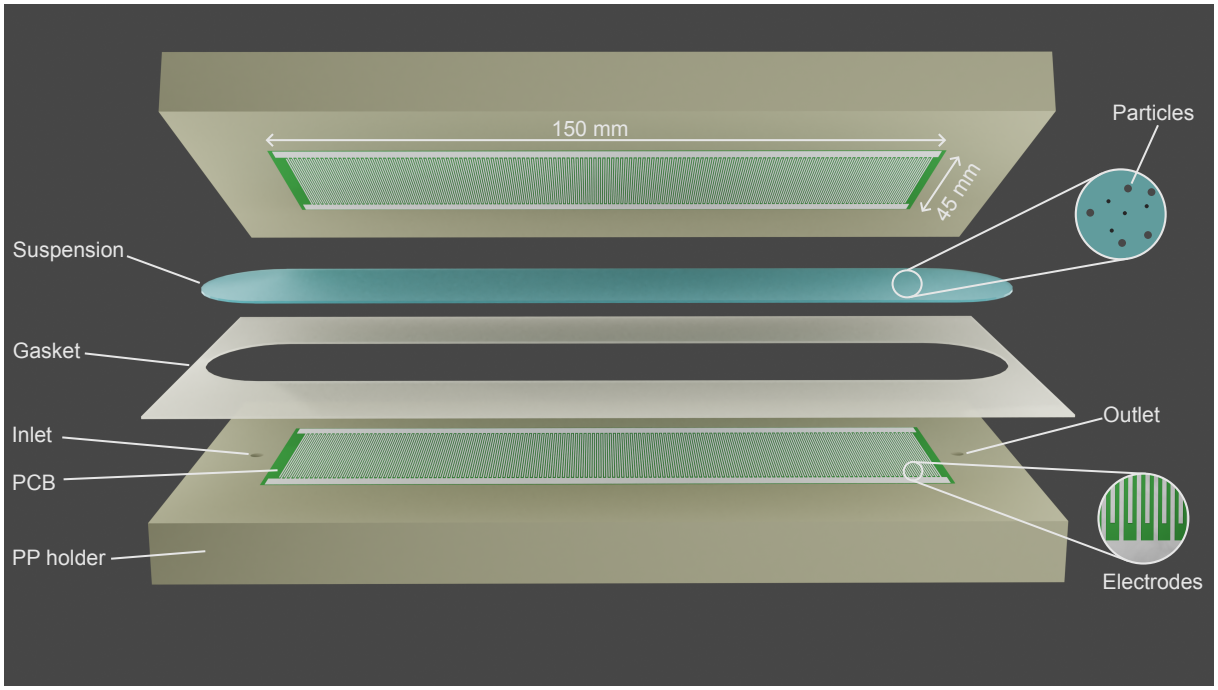

Figure 1: Rendered overview of the separator. The suspension is pumped from inlet to outlet through a channel formed by two printed circuit boards (PCBs), a silicon gasket and the polypropylene (PP) holders. The PCBs feature an interdigitated electrode structure (bottom right insert) that are used to generate a highly inhomogeneous electric field.

(HongKong) Co., Limited, China) with a size of 45 × 150 mm, which is slightly different from the previous design.[23] The improved design showed better performance with reduced PCB size and energy demand. The PCBs are covered by an interdigitated electrode array with an electrode width and spacing both being 250 µm. The two PCBs face each other and are separated by a 0.5 mm silicone gasket. The two PCBs together with the gasket form a channel. The electrodes are connected to a power amplifier (F30PV, Pendulum Instruments, Sweden) which is capable of providing up to 75 V_{pp} at maximum current of 2 A. The sinusoidal signal was generated by a signal generator (Rigol DG4062, Rigol Technologies EU GmbH, Germany), monitored using an oscilloscope (Rigol DS2072A, Rigol Technologies EU GmbH, Germany) and power analyzer (PPA1510, Newtons4th Ltd, Leicester, United Kingdom). The suspension was pumped using a piston pump (Ismatec MCP-CPF IP65 with pump head FMI 202 QP.Q0.SSY, Cole-Parmer GmbH, Germany).

The operating principle is described in detail elsewhere.[23] Briefly, DEP can be an at-

tractive force (positive DEP/pDEP) if a particle is better polarizable than the surrounding medium or a repulsive force (negative DEP/nDEP) when the particle is less polarizable. Positive DEP guides particle towards local field maxima, whereas nDEP pushes particles away from them.[15] This can lead to a separation as was previously shown several times.[23,26,27] Whether a particle experiences pDEP or nDEP depends on the real-part of the Clausius-Mossotti factor (CM), which is defined as[15]

$$\mathrm{Re}(CM) = \mathrm{Re}\left(\frac{\tilde{\varepsilon}_\mathrm{p} - \tilde{\varepsilon}_\mathrm{m}}{\tilde{\varepsilon}_\mathrm{p} + 2\tilde{\varepsilon}_\mathrm{m}}\right), \tag{1}$$

with the complex permittivity $\tilde{\varepsilon} = \varepsilon_0\varepsilon_\mathrm{r} - i\frac{\sigma}{\omega}$. The complex permittivity incorporates not only the permittivity ε but also the angular frequency of the electric field ω and the conductivity of a material σ. $\mathrm{Re}(CM)$ is bound between -0.5 and 1.0 and is negative in case of nDEP and positive in case of pDEP. Finally, the DEP force $\mathbf{F}_\mathrm{DEP}$ for a spherical and homogeneous particle can be approximated as

$$\mathbf{F}_\mathrm{DEP} = 2\pi r_\mathrm{p}^3 \varepsilon_\mathrm{m} \mathrm{Re}(CM) \nabla |\mathbf{E}_\mathrm{rms}|^2 \tag{2}$$

with r_p, the radius of the particle, the electric field, $\mathbf{E}_\mathrm{rms}$, and the permittivity of the surrounding medium, ε_m. Conductive particles in a medium with low conductivity, as used in this study, will usually experience pDEP. $\mathbf{F}_\mathrm{DEP}$ is not only depending on the particle and medium polarizability but also on the particle volume (r_p^3) which is important in the following.

Particles

The particles investigated here all are commercially available. We chose $LiFePO_4$ (Nanografi Nano Teknoloji AS, Turkey) as a cathode material, not only because it is widely used for LIBs but also because it is considered to have low toxicity, which makes it more convenient to work with.[11,28,29] $LiFePO_4$ as cathode material is carbon coated to enhance its otherwise

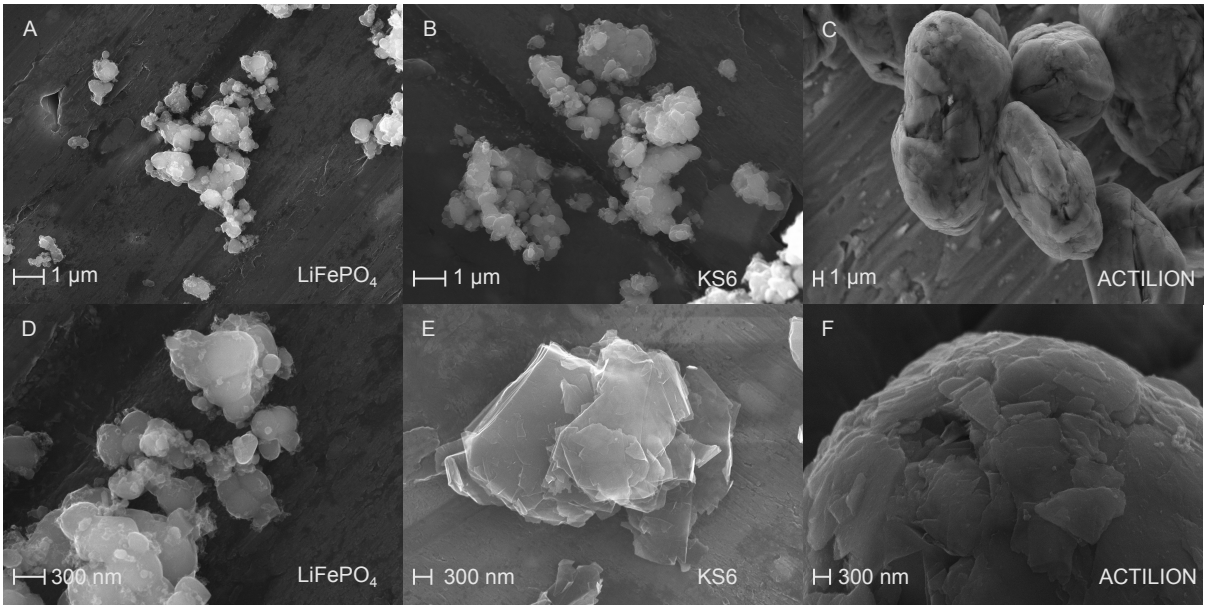

Figure 2: SEM images of $LiFePO_4$ (A&D), KS6 synthetic graphite (B&E) and C-NERGY^{TM} Actilion GHDR 15-4 (C&F) microparticles. The scale bar in the top row equals 1 µm and 300 nm in the bottom row. Please note that the magnification and consequently the scale bar varies in size.

poor conductivity (about 10 nS/cm^{-1}). This leads, according to the distributor, to an electrical conductivity of 0.88 S/m.[30,31] The used $LiFePO_4$ shows a distributed particle size from several hundred nm to a few µm (Table 1, Figure 2 A&D). This is in the range of sizes mentioned in the literature[32–35] and also in the range of the size reported for some other cathode materials.[36] Additionally, two types of graphite particles where selected. Timrex KS6 (MSE Supplies LLC, USA) is a synthetic graphite with high purity which can be used as conductive additive for anodes and cathodes. According to the manufacturer (Imerys Graphite & Carbon, Switzerland), it is larger than the $LiFePO_4$ particles (Table 1, Figure 2 B&E). The second type of graphite C-NERGYTM Actilion GHDR 15-4 (provided by Imerys Graphite & Carbon, Switzerland), here referred to as Actilion, is an active material for anodes of LIBs and significantly larger than the other two materials (Table 1, Figure 2 C&F). The larger size of anode graphite was also described in the literature.[10,11,35] Both graphite and LFP are highly conductive compared to the suspension and thus will show pDEP at all frequencies used in this study. Therefore, all particles will move towards field

maxima which are located at the edges of the electrode array on the PCBs. As the sizes of the particles here diverge significantly, we aim to exploit the linear volume dependence of $\mathbf{F}_{\mathrm{DEP}}$ to achieve a separation.

Table 1: Parameters describing the size distribution of the used particles

Particle	d_{10} / µm	d_{50} / µm	d_{90} / µm
$LiFePO_4$	0.6	1.5	6.0
KS6	1.5	3.4	6.1
Actilion	13	17	23

Measurement system

Two methods were used to measure the particle separation. Qualitatively, the total particle concentration was measured by white-light reflection in real-time at the outlet. Quantitatively, the $LiFePO_4$ concentration was further evaluated using photometric detection of dissolved iron mass. The reflection measurement system is described in Ref. 23. Briefly, it consists of a spectrometer (Silver nova, StellarNet, Inc., USA) and a flow cuvette (176-765-85-40 and 176-760-85-40, Hellma GmbH & Co. KG, Germany). A white light source (XCite 120 PC, Excelitas Technologies Corp., USA) is connected in 90° with respect to the light guide of the spectrometer. Particles in the flow cuvette will scatter the light and produce a signal that can be recorded by the spectrometer. For size-distributed particle systems, it is important to keep in mind that the reflection intensity varies with particle size. For spheres in the size range of the particles used here and the wavelength of the light source, the scattering intensity is proportional to r_{p}^2.[37] As the particles here are not perfect spheres (Figure 2), the signal recorded by the spectrometer does not provide the information of the number or mass of eluted particles, which is different compared to monodisperse particulate systems as in Ref. 23 and 20. This certainly is a downside of the reflection measurement setup. We thus use the measured reflective light intensity reduction at the outlet as a qualitative real-time indicator of particle retention. To measure the retention of $LiFePO_4$ in the filter, we used a chemical procedure which allows a photometric determination of the iron

mass. The procedure was derived from DIN 38406 (see supporting information S5). Briefly, the $LiFePO_4$ particles are dissolved in an acid and the iron content is determined using a complexing agent and performing a photometric measurement afterward.[38]

Experimental procedure

Experiments were carried out in a low-conductivity medium (2.1 µS/cm) consisting of pure water (Omniatap 6 UV/UF, stakpure GmbH, Germany), 0.01 vol.% Tween 20 (Sigma–Aldrich, Germany), and KCl to adjust the conductivity. To create particle stock suspensions, the particles were suspended in an 1 vol.% aqueous Tween 20 suspension with 4 g/L for $LiFePO_4$ and KS6 and 12 g/L for Actilion. The $LiFePO_4$ suspension was renewed every three days as Li is known to dissolve to a low extend into aqueous solutions,[39] and we wanted to exclude this effect from our experiments. Prior to the experiments, we sonicated the particle stock suspensions and added 0.22 vol.% of it, for $LiFePO_4$ and KS6, into the medium for the experiments. In order to achieve a sufficient reflection signal, we had to increase the Actilion concentration, resulting in a 10× higher total mass of Actilion in the final suspension compared to the other two particle types. The reason behind this might be lower specific surface area of the larger Actilion particles and thus lower reflectance per added mass.

The suspensions were stirred throughout the entire experiment. To subtract the background signal, we recorded the intensity signal daily with no particles present (supporting information S2). At the beginning of the experiments we measured the initial reflection signal of the particle suspension for 30 s. At 30 s the electric field was turned on for 270 s. After the voltage was turned off, the experiment was further monitored until the initial intensity was obtained again. Sometimes, the initial signal was not fully reached due to effects such as sedimentation or bubble adhesion in the flow-through cuvette. As a consequence we flushed the entire setup at a high flow rate after every two experiments. Every data point represents three experiments. Equation 1 in section S1 of the supplement details how the signal reduction is calculated.

To chemically determine the retention of the $LiFePO_4$ particles, we collected 4 mL of suspension in a 5 mL container. The samples were taken at the beginning of the experiment, starting after 5 s and during the trapping, starting after 200 s. In order to obtain a sufficient sample volume at the beginning of the experiment, the voltage was turned on after 60 s.

All data from the reflection measurements, the evaluation script (MATLAB, details see supporting information S1) and PCB manufacturing data are uploaded to an online repository (Ref. 40).

Results and Discussion

Frequency dependent behavior up to 500 kHz

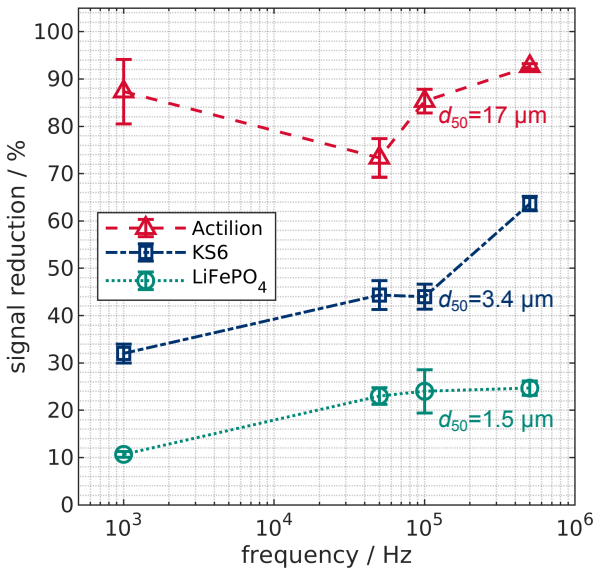

Figure 3: Frequency dependency of the signal reduction of Acilion, KS6 and $LiFePO_4$ suspensions at 6 $mLmin^{-1}$ and 30 V_{pp}. Frequencies were varied between 1 kHz and 500 kHz.

All particles in this study are conductive and thus should show pDEP. To test this hypothesis, we conducted experiments at 30 V_{pp} from 1 kHz to 500 kHz at a volume flow of 6 $mLmin^{-1}$ with only one particle type present per experiment (Figure 3). Higher frequencies

were not applicable in this setup and the selected voltage, because the required current would exceed the maximum of the amplifier. For all particles the trapping efficiency (measured qualitatively in terms of reduction of reflective light intensity signal, called signal reduction) was highest at 500 kHz and significantly higher than at lower frequencies. This might be because disturbing electrokinetic effects like AC electroosmosis can be dominant at lower frequencies.[41] Furthermore, significant difference in the signal reduction becomes apparent when comparing the particle types. This is likely caused by the differences in particles size as DEP scales with particle volume (Equation 2). For example, at 30 V_{pp} and 500 kHz, Actilion shows a high signal reduction of 92.67 ± 0.58 % but the signal of $LiFePO_4$ is only reduced by 24.67 ± 1.53 %. To further investigate the behavior of the particles, we selected 500 kHz as frequency for all subsequent experiments, because the performance of the device is the highest at this frequency and DEP the dominating force. The application of 500 kHz also demonstrates that frequencies in this range can be applied in a high throughput device. A higher possible frequency can be beneficial when designing the process as with increasing frequency the polarizability can alter and enable a separation. In a previous study we could show that retention due to nDEP is small (< 10 %) in such a setup and therefore is not the reason for our observations.[23]

Influence of voltage and volume flow

As second step, we investigated the influence voltage on signal reduction from 5 to 75 V_{pp} at 6 $mLmin^{-1}$ (Figure 4A) and 10 $mLmin^{-1}$ (Figure 4B). At both flow rates, all particles show an increased signal reduction or particle retention with increasing voltage. This is in line with the approximation of the DEP force (Equation 2). Additionally, increasing volume flow decreases the signal reduction. This is due to the increased viscous drag and decreased residence time in the setup at the higher flow rate. The data at 6 $mLmin^{-1}$ and 30 V_{pp} is the same as in Figure 3, except for Actilion. Here, we used a different flow cuvette for this measurements to prevent sedimentation. However, the results are quite similar (here

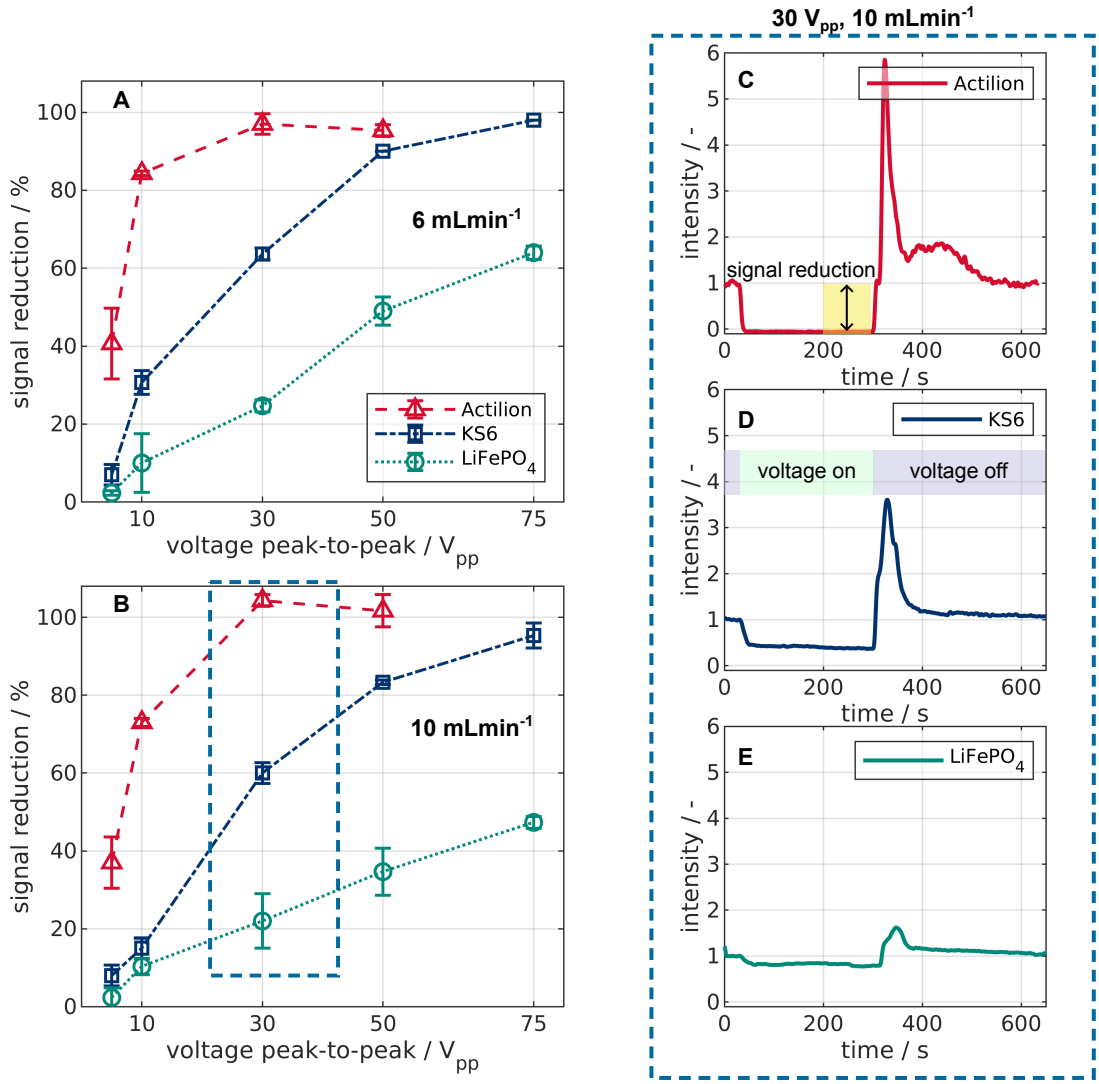

Figure 4: Voltage and volume flow dependency of the signal reduction for Acitlion, KS6 and $LiFePO_4$ suspensions at a frequency of 500 kHz. The behavior was evaluated between 5 and 75 V_{pp} at 6 $mLmin^{-1}$ (A) and 10 $mLmin^{-1}$ (B). As example, normalized reflection intensities over time for all materials at 30 V_{pp} and 10 $mLmin^{-1}$ are also shown (C-E). For all experiments, the signal reduction was measured between 200 and 300 s (C). The voltage was applied after 30 s for 270 s (D).

97 ± 2.65 % compared to 92.67 ± 0.58 %). Figure 4 C-E shows intensity plots over time for all particles at 30 V_{pp} and 10 mLmin^{-1}. Three things become apparent from Figure 4. First, the signal reduction of Actilion is significantly higher than that of $LiFePO_4$. For example, at 30 V_{pp} and 10 mLmin^{-1} (Figure 4 B,C and E), the signal reduction of Actilion is over four times higher than it is for $LiFePO_4$. Here, the recorded intensity for Actilion is close to zero, indicating a complete removal. The relative difference of the signal reduction of $LiFePO_4$ and Actilion, however, decreases with increasing voltage (Figure 4A and B). Likely, this is because Actilion is already almost completely removed at voltages over 30 V_{pp} at both flow rates, whereas $LiFePO_4$ removal increases with voltage from 0 to 75 V_{pp}. Second, KS6 also shows significant trapping and gets fully removed at about 75 V_{pp} at both flow rates. Third, the reflection measurements can create signal reduction slightly higher than 100 % which is linked to the subtraction of the background signal and was observed before.[23] The highest recorded value was $104.33 \pm 1.53\%$ at 10 mLmin^{-1} and 30 V_{pp}. As the deviation is explainable (supporting information S2), relatively small, and showing a complete removal of Actilion, we do not consider this problematic.

In summary, the size, voltage, and volume flow dependency of the signal reduction for these particles was as expected. In addition, we observed an almost complete removal of Actilion from the suspension starting at 30 V_{pp}. For mixtures of $LiFePO_4$ and Actilion, this would correspond to a pure fraction of $LiFePO_4$ at the outlet and an enrichment of Actilion within the filter. Higher voltages than 30 V_{pp} would not lead to a significantly increased trapping of Actilion but to more retained $LiFePO_4$. Therefore, we selected 30 V_{pp} for separation experiments of Actilion and $LiFePO_4$.

Behavior in a mixture of graphite and $LiFePO_4$

As a final step, we investigated the separability of a mixture of $LiFePO_4$ and Actilion. We did not include KS6 because conductive additives are only around 4 % of the battery mass.[2] It would further increase the difficulty of analyzing the results because the reflection

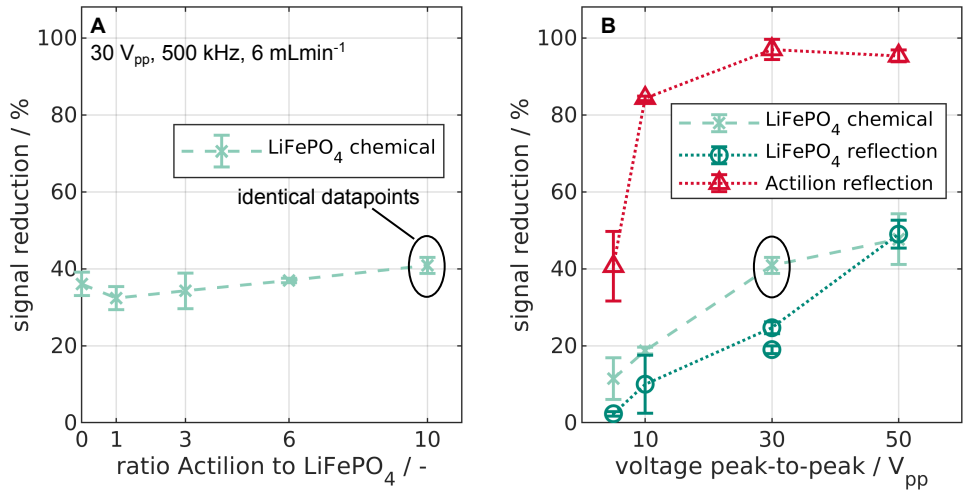

Figure 5: A: Variation of the mass ratio of $LiFePO_4$ and Actilion graphite particles in the suspension at 30 V_{pp}, 500 kHz and 6mLmin^{-1}. B: Comparison of reflection measurements of suspensions with only one particle type present (dotted lines) and the chemical analysis of $LiFePO_4$ removal from a mixture with 10 times more mass of Actilion than $LiFePO_4$ (dashed line).

measurement is not material sensitive. We tried to calculate separate reflection spectra for each component by superposition of the reflection spectra of pure $LiFePO_4$ and Actilion, as they are slightly different. For fluorescent particles this can be achieved by coupling these reference spectra with a global optimization to calculate separate intensities over time distributions as described in Ref. 22. Unfortunately, the results were not reliable for this mixture. Therefore, we had to rely on the information drawn from the experiments with only one particle type present (Figure 3 and 4). To determine the removal of $LiFePO_4$ from the mixture, we performed an additional chemical analysis of the mixture to measure the iron content. Prior to experiments with both particle types present, we compared the chemical and reflection based method using 6 mLmin^{-1}, 500 kHz, and 30 V_{pp} with only $LiFePO_4$ particles in our suspension. The reflection measurement revealed a signal reduction of 19 ± 1 % (Figure 5B: $LiFePO_4$ reflection at 30 V_{pp}) whereas the chemical analysis showed a removal of 36.1 ± 3.04 % (Figure 5A: ratio of 0). Please note, two slightly different signal reductions of two experimental runs, each representing three experiments, at 30 V_{pp} and 6 mLmin^{-1} are shown (Figure 5B). One set of measurements showed a signal reduction

of 24.7 ± 1.5 %, whereas the other were at 19 ± 1 %. We collected the samples for the chemical analysis from the very same experiments in which we recorded the 19 ± 1 % signal reduction. It is therefore reasonable to compare these two values. The difference between chemical analysis and reflection measurement can be explained by the different principles of measurement. While the chemical analysis is measuring the mass of iron, the reflection does correspond to the particle surface area. Larger $LiFePO_4$ particles have high volume and mass but low specific surface area. Due to their large size and thus higher DEP force, they are likely to be retained whereas smaller particles are eluted and detected by the spectrometer. As the smaller particles have a higher specific surface area, they show higher reflection per mass. Consequently, these two measurement techniques are likely to obtain different yet valid results. In the supporting information in section S4, we provide more data, including calculations concerning the mass- and surface-weighted distributions of the $LiFePO_4$ material, which can explain the deviation.

Additionally, we conducted a series of experiments to investigate the influence of the mass ratio of Actilion and $LiFePO_4$ (Figure 5A). The ratio is defined as $m_{\mathrm{Actilion}}/m_{\mathrm{LiFePO_4}}$. The mass ratio does not influence the retention significantly at our set of parameters. Assuming a complete removal of graphite above 30 V_{pp} as measured for the pure graphite, we can assume an almost pure fraction of $LiFePO_4$ at the outlet at voltages above 30 V_{pp} and a retention of about 35 % to 40 % by mass of the $LiFePO_4$ in the filter.

The encircled data in point Figure 5A is also shown in Figure 5B in comparison with results at other voltages. We included the reflection data from Figure 4A of pure Actilion and $LiFePO_4$ for comparison (dotted lines). The chemical analysis again shows an increasing retention of $LiFePO_4$ with voltage (Figure 5B) as it was observed before. Consequently, the conclusions drawn from the suspensions with only one particle type present remain valid, meaning that higher voltages than 30 V_{pp} would not enhance the separation any further. It is likely that the retention of Actilion in the mixed sample is similar to the previously measured retention of pure Actilion, mainly because of two effects. First, we could not

observe any saturation effects within our experiments. Even after almost 1000 s of trapping the signal remained constant (supporting information S3). Second, the addition of $LiFePO_4$ particles could even increase the trapping efficiency. This is because trapped particles can create additional field inhomogeneous that would increase trapping efficiency by forming so-called pearl chains.[42] Nonetheless, the results would benefit from a further investigation of the particles and their mixture before and after the separation to show which particle sizes are retained in the channel and whether there is a cut-off diameter. Also, it needs to be investigated how residuals on the particles (e.g., binder or electrolyte) interfere with the DEP behavior of the particles and what space-time yield this method can achieve. However, this is beyond the scope of this study.

Concluding, we presented the first study on separation of commercially available electrode active materials using dielectrophoresis. The sorting of the particles could lead towards a direct recycling step that can be combined with other recycling techniques which than can reduce the amount of chemicals or energy needed. The results strengthen the assumption that separability using DEP increases with the difference in particle size. As some cathode active materials are even smaller than the $LiFePO_4$ used in this study,[36] it is worth investigating this pathway of recycling further. DEP can also be an option for larger cathode active materials, since the separation could be improved by selective removal of the graphite (several nm thickness[30]) from the cathode particles while not dissolving the anode graphite in the black mass completely. This would decrease the conductivity of the cathode particles and result in weaker pDEP or even nDEP response of the particles and therefore allows material- rather than size-selective separation. With this study, we gave a starting point to direct future research on direct recycling of particle systems using dielectrophresis. We further demonstrated the applicability of dielectrophresis aside from microfluidic applications.

Abbreviations

CM - Clausius-Mossotti factor

DEP - Dielectrophoresis

LIB - Lithium-ion battery

nDEP - negative Dielectrophoresis

PCB - printed circuit board

pDEP - positive Dielectrophoresis

Acknowledgment

The authors thank the German Research Foundation (DFG) within the priority program, "MehrDimPart—Highly specific and multidimensional fractionation of fine particle systems with technical relevance" (SPP2045, Grant Numbers PE 3015/3-2, TH 893/20-2) for funding. We also thank Krischan Sandmann and Dilyan Kamenov from the IWT Bremen for helping to conduct particle size analysis.

References

(1) Lv, W.; Wang, Z.; Cao, H.; Sun, Y.; Zhang, Y.; Sun, Z. A Critical Review and Analysis on the Recycling of Spent Lithium-Ion Batteries. *ACS Sustainable Chemistry & Engineering* **2018**, *6*, 1504–1521.

(2) Natarajan, S.; Divya, M. L.; Aravindan, V. Should We Recycle the Graphite from Spent Lithium-Ion Batteries? The Untold Story of Graphite with the Importance of Recycling. *Journal of Energy Chemistry* **2022**, *71*, 351–369.

(3) Wu, X.; Ma, J.; Wang, J.; Zhang, X.; Zhou, G.; Liang, Z. Progress, Key Issues, and Future Prospects for Li-Ion Battery Recycling. *Global Challenges* **2022**, *6*, 2200067.

(4) Neumann, J.; Petranikova, M.; Meeus, M.; Gamarra, J. D.; Younesi, R.; Winter, M.; Nowak, S. Recycling of Lithium-Ion Batteries—Current State of the Art, Circular Economy, and Next Generation Recycling. *Advanced Energy Materials* **2022**, *12*, 2102917.

(5) Vanderbruggen, A.; Hayagan, N.; Bachmann, K.; Ferreira, A.; Werner, D.; Horn, D.; Peuker, U.; Serna-Guerrero, R.; Rudolph, M. Lithium-Ion Battery Recycling-Influence of Recycling Processes on Component Liberation and Flotation Separation Efficiency. *ACS ES&T Engineering* **2022**,

(6) Abdollahifar, M.; Doose, S.; Cavers, H.; Kwade, A. Graphite Recycling from End-of-Life Lithium-Ion Batteries: Processes and Applications. *Advanced Materials Technologies* *n/a*, 2200368.

(7) Werner, D.; Peuker, U. A.; Mütze, T. Recycling Chain for Spent Lithium-Ion Batteries. *Metals* **2020**, *10*, 316.

(8) Heath, G. A.; Ravikumar, D.; Hansen, B.; Kupets, E. A Critical Review of the Circular Economy for Lithium-Ion Batteries and Photovoltaic Modules – Status, Challenges, and Opportunities. *Journal of the Air & Waste Management Association* **2022**, *72*, 478–539.

(9) Satyavani, T. V. S. L.; Ramya Kiran, B.; Rajesh Kumar, V.; Srinivas Kumar, A.; Naidu, S. V. Effect of Particle Size on Dc Conductivity, Activation Energy and Diffusion Coefficient of Lithium Iron Phosphate in Li-ion Cells. *Engineering Science and Technology, an International Journal* **2016**, *19*, 40–44.

(10) Dai, K.; Wang, Z.; Ai, G.; Zhao, H.; Yuan, W.; Song, X.; Battaglia, V.; Sun, C.; Wu, K.; Liu, G. The Transformation of Graphite Electrode Materials in Lithium-Ion Batteries after Cycling. *Journal of Power Sources* **2015**, *298*, 349–354.

(11) Kassem, M.; Delacourt, C. Postmortem Analysis of Calendar-Aged Graphite/LiFePO4 Cells. *Journal of Power Sources* **2013**, *235*, 159–171.

(12) Vanderbruggen, A.; Salces, A.; Ferreira, A.; Rudolph, M.; Serna-Guerrero, R. Improving Separation Efficiency in End-of-Life Lithium-Ion Batteries Flotation Using Attrition Pre-Treatment. *Minerals* **2022**, *12*, 72.

(13) Zhan, R.; Oldenburg, Z.; Pan, L. Recovery of Active Cathode Materials from Lithium-Ion Batteries Using Froth Flotation. *Sustainable Materials and Technologies* **2018**, *17*, e00062.

(14) Harper, G.; Sommerville, R.; Kendrick, E.; Driscoll, L.; Slater, P.; Stolkin, R.; Walton, A.; Christensen, P.; Heidrich, O.; Lambert, S.; Abbott, A.; Ryder, K.; Gaines, L.; Anderson, P. Recycling Lithium-Ion Batteries from Electric Vehicles. *Nature* **2019**, *575*, 75–86.

(15) Pethig, R. Review Article—Dielectrophoresis: Status of the Theory, Technology, and Applications. *Biomicrofluidics* **2010**, *4*, 022811.

(16) Pesch, G. R.; Du, F. A Review of Dielectrophoretic Separation and Classification of Non-biological Particles. *ELECTROPHORESIS* **2021**, *42*, 134–152.

(17) *Dielectrophoresis*; John Wiley & Sons, Ltd: Chichester, UK, 2017; pp 309–379.

(18) Balasubramanian, P.; Kinders, R. J.; Kummar, S.; Gupta, V.; Hasegawa, D.; Menachery, A.; Lawrence, S. M.; Wang, L.; Ferry-Galow, K.; Davis, D.; Parchment, R. E.; Tomaszewski, J. E.; Doroshow, J. H. Antibody-Independent Capture of Circulating Tumor Cells of Non-Epithelial Origin with the ApoStream® System. *PLOS ONE* **2017**, *12*, e0175414.

(19) Sano, H.; Kabata, H.; Kurosawa, O.; Washizu, M. Dielectrophoretic Chromatography with Cross-Flow Injection. Technical Digest. MEMS 2002 IEEE International Conference. Fifteenth IEEE International Conference on Micro Electro Mechanical Systems (Cat. No.02CH37266). Las Vegas, NV, USA, 2002; pp 11–14.

(20) Lorenz, M.; Malangré, D.; Du, F.; Baune, M.; Thöming, J.; Pesch, G. R. High-Throughput Dielectrophoretic Filtration of Sub-Micron and Micro Particles in Macroscopic Porous Materials. *Analytical and Bioanalytical Chemistry* **2020**, *412*, 3903–3914.

(21) Pesch, G. R.; Lorenz, M.; Sachdev, S.; Salameh, S.; Du, F.; Baune, M.; Boukany, P. E.; Thöming, J. Bridging the Scales in High-Throughput Dielectrophoretic (Bio-)Particle Separation in Porous Media. *Scientific Reports* **2018**, *8*, 10480.

(22) Weirauch, L.; Giesler, J.; Baune, M.; Pesch, G. R.; Thöming, J. Shape-Selective Remobilization of Microparticles in a Mesh-Based DEP Filter at High Throughput. *Separation and Purification Technology* **2022**, *300*, 121792.

(23) Giesler, J.; Weirauch, L.; Thöming, J.; Baune, M.; Pesch, G. R. High-Throughput Dielectrophoretic Separator Based on Printed Circuit Boards. *ELECTROPHORESIS* **2023**, *44*, 72–81.

(24) Shen, Y.; Elele, E.; Khusid, B. A Novel Concept of Dielectrophoretic Engine Oil Filter. *ELECTROPHORESIS* **2011**, *32*, 2559–2568.

(25) Suehiro, J.; Guangbin Zhou,; Imamura, M.; Hara, M. Dielectrophoretic Filter for Separation and Recovery of Biological Cells in Water. *IEEE Transactions on Industry Applications* **2003**, *39*, 1514–1521.

(26) Giesler, J.; Weirauch, L.; Thöming, J.; Baune, M.; Pesch, G. R. Separating Microparticles by Material and Size Using Dielectrophoretic Chromatography with Frequency Modulation. *Scientific Reports* **2021**, *11*, 16861.

(27) Modarres, P.; Tabrizian, M. Frequency Hopping Dielectrophoresis as a New Approach for Microscale Particle and Cell Enrichment. *Sensors and Actuators B: Chemical* **2019**, *286*, 493–500.

(28) Liang, Q.; Yue, H.; Wang, S.; Yang, S.; Lam, K.-h.; Hou, X. Recycling and Crystal Regeneration of Commercial Used LiFePO4 Cathode Materials. *Electrochimica Acta* **2020**, *330*, 135323.

(29) Qiu, X.; Zhang, B.; Xu, Y.; Hu, J.; Deng, W.; Zou, G.; Hou, H.; Yang, Y.; Sun, W.; Hu, Y.; Cao, X.; Ji, X. Enabling the Sustainable Recycling of LiFePO $_4$ from Spent Lithium-Ion Batteries. *Green Chemistry* **2022**, *24*, 2506–2515.

(30) Chen, Z.; Zhang, Q.; Liang, Q. Carbon-Coatings Improve Performance of Li-Ion Battery. *Nanomaterials* **2022**, *12*, 1936.

(31) Doeff, M. M.; Wilcox, J. D.; Kostecki, R.; Lau, G. Optimization of Carbon Coatings on LiFePO4. *Journal of Power Sources* **2006**, *163*, 180–184.

(32) Lepage, D.; Sobh, F.; Kuss, C.; Liang, G.; Schougaard, S. B. Delithiation Kinetics Study of Carbon Coated and Carbon Free LiFePO4. *Journal of Power Sources* **2014**, *256*, 61–65.

(33) Zhang, H.; Wang, L.; Chen, Y.; Wen, X. Regenerated LiFePO4/C for Scrapped Lithium Iron Phosphate Powder Batteries by Pre-Oxidation and Reduction Method. *Ionics* **2022**, *28*, 2125–2133.

(34) Larouche, F.; Amouzegar, K.; Houlachi, G.; Bouchard, P.; Demopoulos, G. P. Conversion of LiFePO $_4$ to FePO $_4$ via Selective Lithium Bicarbonation: A Direct Pathway Towards Battery Recycling. *Journal of The Electrochemical Society* **2022**, *169*, 073509.

(35) Zaghib, K.; Striebel, K.; Guerfi, A.; Shim, J.; Armand, M.; Gauthier, M. LiFePO4/Polymer/Natural Graphite: Low Cost Li-ion Batteries. *Electrochimica Acta* **2004**, *50*, 263–270.

(36) Li, J.; Daniel, C.; Wood, D. Materials Processing for Lithium-Ion Batteries. *Journal of Power Sources* **2011**, *196*, 2452–2460.

(37) Friedlander, S. K. *Smoke, Dust, and Haze: Fundamentals of Aerosol Dynamics*, 2nd ed.; Topics in Chemical Engineering; Oxford University Press: New York, 2000.

(38) DIN 38406 Teil 1 - Deutsche Einheitsverfahren zur Wasser-, Abwasser- und Schlammuntersuchung. 1983.

(39) Porcher, W.; Moreau, P.; Lestriez, B.; Jouanneau, S.; Guyomard, D. Is LiFePO4 Stable in Water?: Toward Greener Li–Ion Batteries. *Electrochemical and Solid-State Letters* **2007**, *11*, A4.

(40) Giesler, J. Online Repository for "Sorting Lithium-Ion Battery Electrode Materials Using Dielectrophoresis at Frequencies of up to 500 kHz". https://doi.org/10.5281/zenodo.7593873, 2023.

(41) Castellanos, A.; Ramos, A.; González, A.; Green, N. G.; Morgan, H. Electrohydrodynamics and Dielectrophoresis in Microsystems: Scaling Laws. *Journal of Physics D: Applied Physics* **2003**, *36*, 2584–2597.

(42) Kong, T. F.; Tan, P. Y.; Tay, B. Z.; Shen, X.; Marcos, Bacteria and Cancer Cell Pearl Chain under Dielectrophoresis. *ELECTROPHORESIS* **2021**, *42*, 1070–1078.